SAND2021-3914C

Stabilization of Generator Frequency Under Pulsed Load Condition Using Regenerative Propeller Braking

Ronald C. Matthews
Electric Power Systems Research
Sandia National Laboratories
Albuquerque, NM, USA
rcmatth@sandia.gov

Lee J. Rashkin
Electrical Science & Experiments
Sandia National Laboratories
Albuquerque, NM, USA
lrashki@sandia.gov

Steve F. Glover
Electrical Science & Experiments
Sandia National Laboratories
Albuquerque, NM, USA
dwilso@sandia.gov

Norbert H. Doerry
Carderock Division
Naval Surface Warfare Center
West Bethesda, MD, USA
norbert.doerry@navy.mil

***Abstract*—In this paper, the effects and mitigation strategies of pulsed loads on medium voltage DC (MVDC) electric ships are explored. Particularly, the effect of high-powered pulsed loads on generator frequency stability are examined. As a method to stabilize a generator which has been made unstable by high-powered pulsed loads, it is proposed to temporarily extract energy from the propulsion system using regenerative propeller braking. The damping effects on generator speed oscillation of this method of control are examined. The impacts on propeller and ship speed are also presented.**

Keywords—regenerative propeller braking, pulsed loads, all-electric warship, control

I. Introduction

As discussed in [1], pulsed loads are becoming more common on Naval ships. Devices such as electromagnetic aircraft launch systems (EMALS), rail guns, lasers, and radar have stochastic load profiles that can vary sharply in time and look like a series of pulses on the system. Such loads have a destabilizing effect on a ships power distribution network.

On shipboard power systems space is limited in terms of the amount of energy storage that can be made available. With the limited available space, minimizing the need for physical energy storage is of great importance. In [2], the Hamiltonian Surface Shaping and Power Flow Control (HSSPFC) design is configured to focus on minimizing physical energy storage requirements. However, once the storage requirements have been minimized, there is still additional potential for extracting power from other more dispatchable loads such as the propellers in an emergency or critical condition.

Additionally, even if sufficient battery storage is available, charging or discharging too rapidly can damage the battery [3]. For high power pulsed loads transient current swings may be extremely rapid. According to [4], although batteries are far more energy dense than flywheels, the power density of a flywheel is up to 10MW/kg whereas electrochemical storage is capable of up to 1 MW/kg [4]. Therefore, flywheels are better suited to respond to the high power, short duration pulses and fast transients. However, the presence of a flywheel requires additional space and mechanical considerations which may not be feasible. As an alternative, the ships propeller is proposed to be used as a combination flywheel/regenerative brake. That is, energy can be pulled directly from the inertia of the propeller itself; and the propeller can be used to pull horizontal inertia from the ship to be used during active load pulses.

Regenerative braking has seen extensive use in recent years in land vehicles to increase efficiency in electric and hybrid electric drive vehicles on land [5, 6]. However, in this paper it is proposed to be applied to large scale seacrafts. In the next section an overview of regenerative braking is discussed as it relates to land vehicles and it is then extended to seacrafts. . The control strategy to enable support for the pulsed loads is described in Section III. Section IV discusses the modelling environment used in this work.

II. Regenerative Braking

As a consequence of heightened interest in energy conservation and combating climate change, electric and hybrid electric vehicles are becoming more commonplace [5, 7]. Such vehicles form complex, self-contained microgrids. An automobile must be able to perform two obvious functions. It must be able to accelerate, and it must be able to brake. Here, the focus is on the latter. In a traditional vehicle, the braking action is performed by converting kinetic energy into friction energy and releasing heat into the environment. However, this is the antitheses of efficiency, since this heat cannot be recovered for future use. As an alternative, electric and hybrid electric vehicles are capable of braking by restoring the vehicles kinetic energy to the battery storage [8]. The same general strategy can be applied to an electric shipboard system.

In this work, a dual-fed induction motor is used to drive the ship's propeller. Various methods exist for controlling an induction motor. However, for this work, volts-per-hertz control is chosen for its simplicity [9]. When an induction motor has a negative slip, it can operate as a generator as described in [6]. The stator electrical frequency is directly controlled by the inverter. This frequency may be changed as desired. Dropping the electrical frequency of the stator below the electrical frequency of the rotor allows the motor to act as a generator and

Sandia National Laboratories is a multimission laboratory managed and operated by National Technology & Engineering Solutions of Sandia, LLC, a wholly owned subsidiary of Honeywell International Inc., for the U.S. Department of Energy's National Nuclear Security Administration under contract DE-NA0003525.

reverse the flow of power back into the inverter. This is the approach utilized here.

III. Ship Speed Control

When controlling a land vehicle, there is a simple relation between the rotational speed of the tires and the forward motion of the vehicle. Tire slippage is relatively small so that it may be neglected when attempting to estimate vehicle speed. The circumference of the wheel directly translates to the vehicles forward motion, even during transients provided the tire does not lose substantial traction. This is the driving principle behind how a common speedometer operates. Assuming the wheel diameter of the vehicle has not been altered and that the tires have not lost substantial traction, the rotational speed of the wheels can accurately be used to determine the horizontal speed of the vehicle [10].

However, on water, slippage of the propeller is far more substantial. A full model of the ship is needed just to estimate the steady state relationship between the propeller speed and the ship's forward speed. For the volts-per-hertz control to be effective, the propeller speed must be directly controlled. However, the propeller frequency does not directly correlate to the horizontal speed during transients. The goal is to control the speed of the ship. This is done using a control scheme which approximately maps the steady state speed of the ship to a specific rotor (propeller) speed. Closed loop feedback control is then used to drive the propeller to the estimated speed target. The relation between desired steady state ship speed and required propeller speed used in this paper is shown below in Fig. 1. This relation can be used to directly control the propeller speed to approximately get to the desired horizontal ship speed.

The volts-per-hertz control scheme is as described in [9] with slight modification. The speed controller is detailed as shown in Fig. 1. The input is the speed of the ship in knots $\boldsymbol{v_{ship}}$. This is transformed via the polynomial defined in Fig. 2. to get the target mechanical propeller speed $\boldsymbol{\omega_{rm}}$. The remainder of the control is the standard volt-per-hertz control which outputs the q- and d-axis voltage references $\boldsymbol{v_{qs}^*}$ and $\boldsymbol{v_{ds}^*}$ along with the angular electrical frequency $\boldsymbol{\omega_e}$ input which is also the target rotor electrical frequency $\boldsymbol{\omega_r^*}$

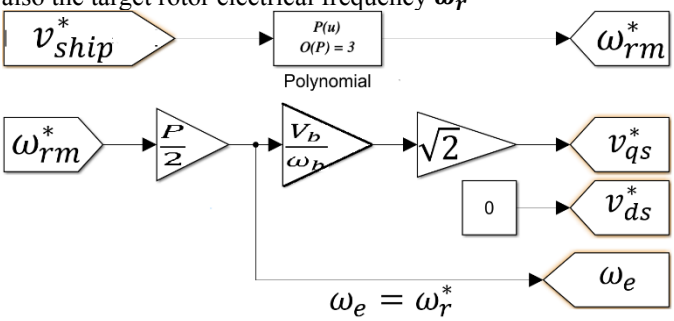

Fig. 1. Modified volts-per-hertz speed controller.

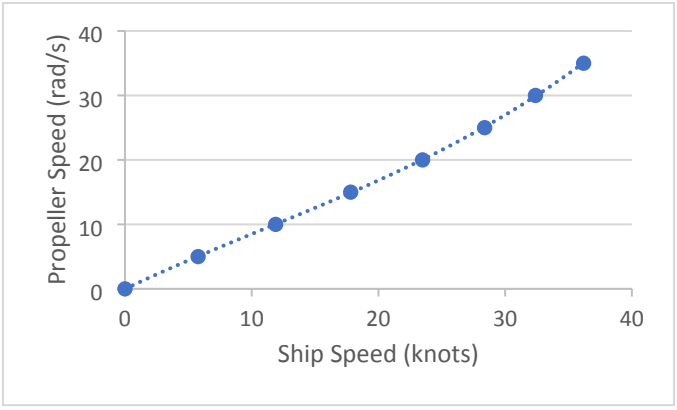

Fig. 2. Propeller rotation-horizontal speed steady-state relation. The horizontal axis is the speed is the velocity of the ship in knots and the vertical axis is the mechanical angular frequency of the propeller in rad/s.

IV. Models

The shipboard system was modelled in Simulink using the SwAGSM modelling tool. This tool allows for a model to be constructed through entries on the model properties and connection in an Excel spreadsheet that can then be used to generate Simulink or OPAL-RT models. This tool was first detailed in one of its earlier versions in [11] and has been further used in modelling and development in [12], [13], and [14]. The shipboard system used in this paper consisted of a battery, dual-wound gas turbine generator, and propulsion models.

A. Battery Model

A Li-Ion battery is modeled as described in [11], [15]. For this example, the battery used the parameters shown in TABLE I. where, V_{nom} is the nominal voltage of the battery, Ah_{rating} is the amp-hour rating of the battery, $\eta_{battery}$ is the battery efficiency, and $SOC(0)$ is the initial state of charge of the battery.

TABLE I. Battery Model Properties

Parameter	Value
V_{nom}	2 kW
Ah_{rating}	300000 Ah
$\eta_{battery}$	99.5%
SOC(0)	80%

B. Generator Model

The generator is a 4.16 kV dual winding generator with a load capacity of 100 MW. The prime mover is a diesel engine and is modeled as described in [16]. The block diagram for this model is shown in Fig. 3. The parameters used here are shown in TABLE II. Where ω is the angular electrical frequency of the rotor. ω_{ref} is the reference angular frequency. T_1,T_2,T_3 are control system time constants. T_4,T_5,T_6 are actuator time constants. T_{min} and T_{max} are the lower and upper per unit torque limit respectively. T_d is the combustion time delay. The generator itself is a dual winding generator as detailed in [17] [14] with a winding separation of 60°.

TABLE II. DIESEL ENGINE MODEL PARAMETERS

Parameter	Value
ω_{ref}	376.9911 rad/s
K	5
T_1	0.01 s
T_2	0.02 s
T_3	0.2 s
T_4	0.25 s
T_5	0.009 s
T_6	0.0384 s
T_{min}	0.0
T_{max}	1.1
T_d	0.024 s

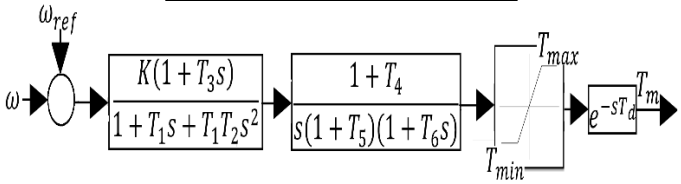

Fig. 3. Block diagram for linearized diesel engine model.

C. Propulsion Model

The 1-dimensional ship propulsion is modeled as detailed in [18] [19] [20]. Let N_p be the propeller speed in rad/s. The propeller speed, n_{prop}, in rev/s becomes

$$n_{prop} = \frac{N_p}{60} \tag{1}$$

Define the propeller second order advance coefficient

$$\sigma = \frac{n_{prop}D_{prop}}{\sqrt{v_p^2 + (n_{prop}D_{prop})^2}} \tag{2}$$

where D_{prop} is the propeller diameter in ft and V_p is the speed of the ship in ft/s. The propeller thrust of the ship is

$$T = c_T(\sigma)\rho_{sw}\, D_{prop}^2\left(V_p^2 + \left(n_{prop}D_{prop}\right)^2\right) \tag{3}$$

and the propeller torque is

$$Q = c_Q(\sigma)\rho_{sw}\, D_{prop}^3\left(V_p^2 + \left(n_{prop}D_{prop}\right)^2\right) \tag{4}$$

The parameter $c_T(\sigma)$ and $c_Q(\sigma)$ are dependent upon the geometry of the ship. The speed of advance is

$$V_p = V(1-w) \tag{5}$$

Where w is the wake fraction and V is the horizontal speed of the ship. The wake fraction $w(v_{ship})$ is dependent on the ship geometry and the speed of the ship. Where v_{ship} is the actual horizontal speed of the ship. Also define

$$T_p = T(1-t) \tag{6}$$

where T is the propeller torque, and t is the thrust deduction factor

The speed of the ship is then

$$M\frac{dv_{ship}}{dt} = T - R_T \tag{7}$$

where, $R_T(v_{ship})$ is the total hull resistance, and M is the mass of the ship. For this example, the total ship mass is 30,060 slugs, the propeller diameter is 15 ft, and the propeller inertia is 55277.3 $kg\ m^2$.

V. RESULTS

The 8-bus network shown in Fig. 4 is considered. The total generation capability is 100 MW. The pulse load is at bus 7. The 33 MW pulse train has a period of 2s with a duty cycle of 0.25s (12.5%).

The port and starboard buses are to the far left and far right respectively. These are both nominal 12 kV. The pulse load operates at a nominal 6 kV. The total rotational inertia of the generator is 256.38 $kg\ m^2$.

A. Case 1: 33 MW Pulse Train without Frequency Correction

It can be seen in Fig. 5 that the propeller frequency is constant at about 16.56 rad/s once steady state is reached and is unaffected by the pulsed load. The power at steady state to maintain the 19.65 knots steady state speed is about 6.95 MW as can be seen in Fig. 6. The ship speed is shown in Fig. 7.

The dual-wound generator frequency is shown in the top curve of Fig. 8. Hard frequency dips can be seen every 2 seconds when the pulsed load becomes active. The pulsed load appears to be making the generator frequency unstable since the dips seems to be increasing over time. This is because the pulses are pulling energy from the generator faster than its controls can manage casing it to decelerate. Then, when the pulsed end, the generator rapidly accelerates. This back and forth overshot-undershoot compounds in the generator and eventually leads to frequency collapse as can be seen in Fig. 8. The lower frequency in the figure is the electrical frequency of the dual-fed induction motor rotor which settles at about 250 rad/s over the duration of the simulation.

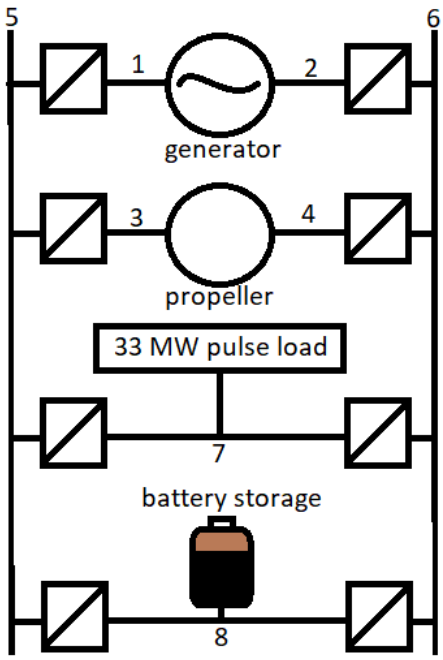

Fig. 4. 8-Bus Shipboard System.

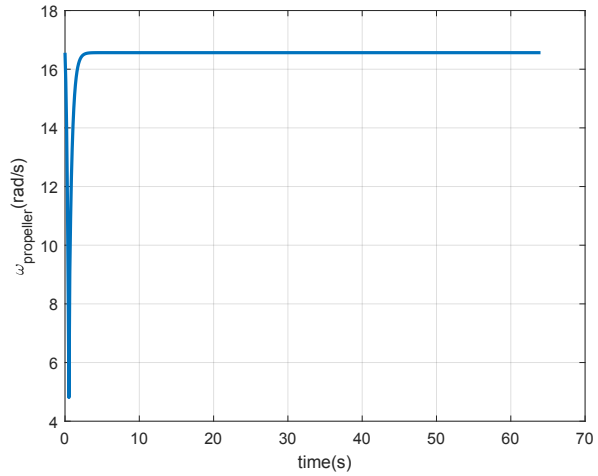

Fig. 5. Propeller Speed.

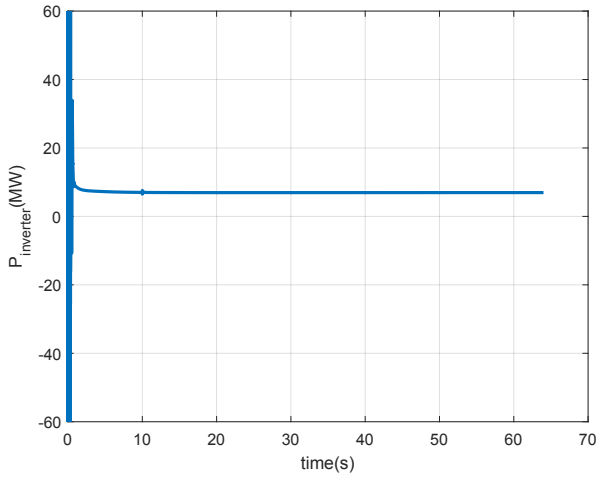

Fig. 6. Power into speed control inverter.

B. Case 2: 33 MW Pulse Train with Frequency Correction

In this case, all conditions and parameters are identical to Case 1. However, the propeller attempts to brake the ship to reduce its speed when the 33 MW pulse occurs. This is done by temporarily setting the ships target speed to zero so that the ship pulls energy from the propeller's kinetic energy to feed the pulsed load while it is active. The underlying assumption here is that communication exists between the propeller's controls and the pulse load so that regenerative propeller braking is triggered when the pulse is active and is disable when the pulse in on standby. That is, the load pulse timing is perfectly know by the controller. It should be noted here that this control scheme is only valid for a single pulse. Moreover, if the pulse load is too long, the propeller will lose all its inertia eventually rendering the scheme ineffective. For longer pulses or multiple pulses, other frequency correction schemes need to be explored. This is a topic which will be explored in future work.

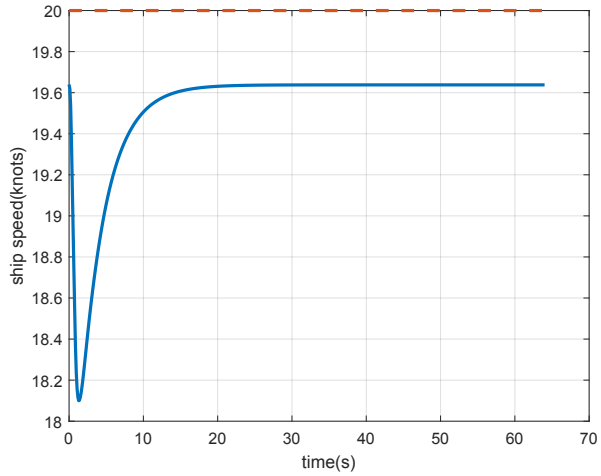

Fig. 7. Ship Speed.

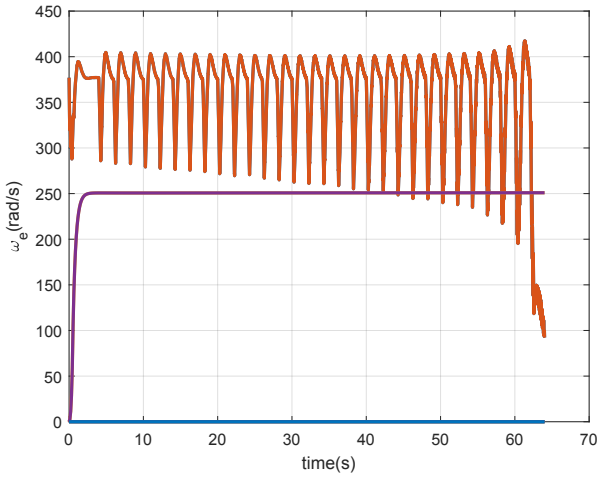

Fig. 8. Electrical Frequencies where (orange) Dual-wound generator speed, (purple) propulsion speed.

The propeller speed is shown in Fig. 9. The propeller speed peaks is at the same 16.56 rad/s as in Case 1. However, the propeller loans its stored rotating inertia to aid in stabilizing the generator frequency when the pulse is active. The propeller dips to about 8.2 rad/s when the pulse becomes active to counter its effects on the generator frequency.

It can be seen in Fig. 10 that the inverter pulls a peak power of about 50 MW from the propeller when the pulsed loads become active. This additional energy both stabilizes the frequency oscillations and reduces the magnitude of the oscillations. With regenerative propeller braking, the frequency oscillations are limited to between 355 and 387 rad/s. This is a drastic improvement over the unstable oscillations seen in Case 1. The dual-fed induction motor rotor electrical frequency peaks at the same 250 rad/s as in Case 1 and dips to about 120 rad/s when the pulse become active. This can be observed in Fig. 11.

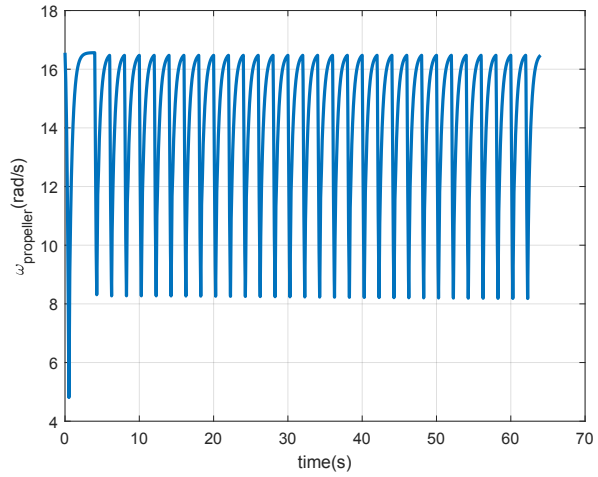

Fig. 9. Propeller speed.

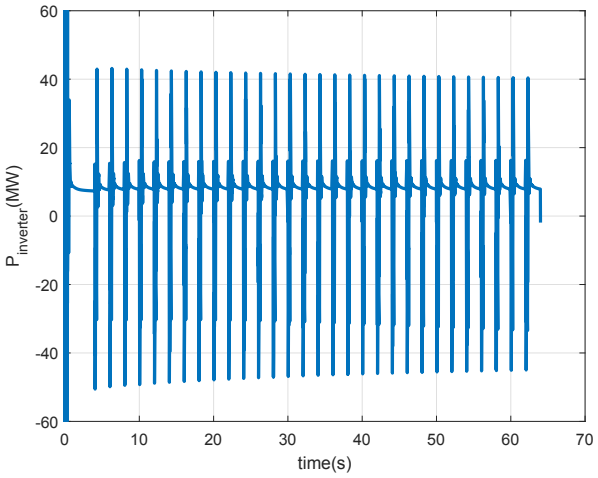

Fig. 10. Power into speed controller inverter.

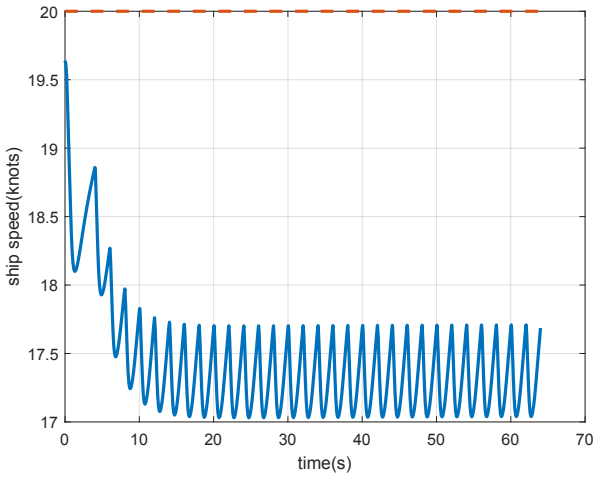

Fig. 11. Ship speed.

As a consequence of the enhanced frequency stability, the ship speed performance does suffer slightly. The speed drop from the steady state value of 19.65 knots to oscillate between about 17 and 17.8 knots as can be seen in Fig. 12. The period of the oscillations is relatively slow (2 seconds). However, the effects of horizontal speed oscillations on the human crew requires additional research beyond the scope of this paper.

VI. Conclusion

Overall, it was found that drawing power from the ships forward and rotating inertia using regenerative braking of the propeller can drastically enhance generator frequency stability. The cost is small in that there will be a slight dip in the average speed of the ship and the speed will become oscillatory.

It was assumed that the pulse timing was perfectly known to the speed controller so that it may act accordingly. However, it may be the case that communication is not available between the pulsed load and the propulsion controller (inverter). Additionally, even if this information is known, there may be multiple pulses firing at different times, durations, and power levels. These are topics which will be explored in future work.

Acknowledgment

Sandia National Laboratories is a multimission laboratory managed and operated by National Technology & Engineering Solutions of Sandia, LLC, a wholly owned subsidiary of Honeywell International Inc., for the U.S. Department of Energy's National Nuclear Security Administration under contract DE-NA0003525. This paper describes objective technical results and analysis. Any subjective views or opinions that might be expressed in the paper do not necessarily represent the views of the U.S. Department of Energy or the United States Government. This paper was approved for release as SAND XXXXX.

This work was supported by NAVSEA Naval Power Systems, Electric Ship PMS 320 program for a project entitled Nonlinear Power Flow Control Design for NGIP Energy Storage Requirements, PR# 1400354102. In addition, the authors would like to thank the director of the program, Stephen Markle and his team.

Distribution Statement A: Approved for public release: distribution unlimited.

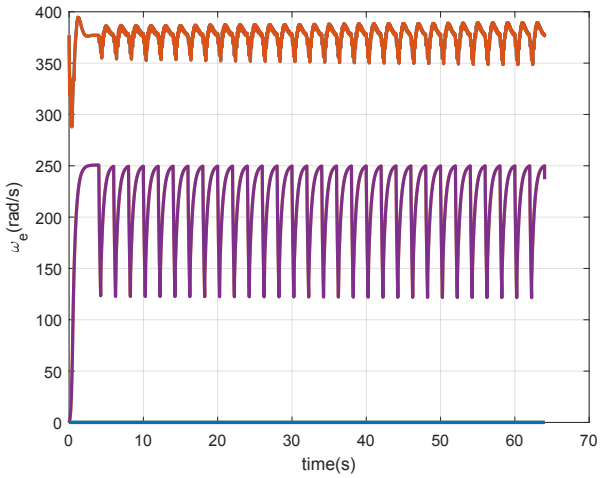

Fig. 12. Electrical Frequencies where (orange) Dual-wound generator speed, (purple) propulsion speed

References

[1] W. W. Weaver and D. G. W. R. C. M. Rush D. Robinett III, "Metastability of Pulse Power Loads Using the Hamiltonian Surface Shaping Method," *IEEE Transactions on Energy Conversion,* vol. 32, no. 2, pp. 820-828, 2017.

[2] D. G. Wilson, R. D. R. II, W. W. Weaver, R. H. Byrne and J. Young, "Nonlinear Power Flow Control Design of High Penetration Renewable," in *International Symposium on Power Electronics, Electrical Drives, Automation and Motion*, Capri, 2016.

[3] C. Sinkaram, K. Rajakumar and V. Asirvadam, "Modeling Battery Management System Using The Lithium-Ion Battery," in *2012 IEEE International Conference on Control System, Computing and Engineering*, Penang, 2012.

[4] H. Ibrahim and A. Ilinca, Techno-Economic Analysis of Different Energy Storage Technologies, Energy Storage - Technologies and Applications, London: IntechOpen, 2013.

[5] G. Mishra and J. Choudhari, "Energy Harvesting with Regenerative Braking for Induction Motor," in *Proceedings of the 2nd International conference on Electronics, Communication and Aerospace Technology*, Coimbatore, 2018.

[6] P. B. Mohan and V. R. Bindu, "Energy Regeneration in Induction Machine Energy Regeneration in Induction Machine Drive during Braking," in *2nd International Conference on Trends in Electronics and Informatics (ICOEI 2018)*, Tirunelveli, 2018.

[7] P. B. Mohan and V. R. Bindu, "Energy Regeneration in Induction Machine Drive during Braking," in *2nd International Conference on Trends in Electronics and Informatics (ICOEI 2018)*, Cheranmahadevi, 2018.

[8] S. Cholula, A. Claudio and J. Ruiz, "Intellegent Control of the Regenerative Braking in an Induction Motor Drive," in *2nd International Conference on Electrical and Electronic Engineering (ICEEE)*, Mexico City, 2005.

[9] P. C. Krause, O. Wasynczuk and S. D. Sudhoff, Analysis of Electric Machinery and Drive Systems, Piscataway: IEEE Press, 2002.

[10] C. Murray, "Wheel Diameter and Speedometer Reading," *The Physics Teacher,* vol. 48, pp. 416-418, 2010.

[11] R. C. Matthews, "Power flow control in hybrid ac/dc microgrids," Michigan Technological University, Houghton, 2018.

[12] R. Matthews, W. Weaver, R. Robinett and D. Wilson, "Hamiltonian methods of modeling and control of AC microgrids with spinning machines and inverters," *International Journal of Electrical Power and Energy Systems,* vol. 98, pp. 315-322, 2018.

[13] R. Jane, G. Parker, W. Weaver, R. Matthews, D. Rizzo and M. Cook, "Optimal Power Management of Vehicle Sourced Military Outposts," *SAE International Journal of Commercial Vehicles,* vol. 10, no. 1, pp. 132-143, 2017.

[14] L. Rashkin, R. Matthews, J. Neely and N. Doerry, "Dynamic Response Comparison of Dual-Wound and Single-Wound Machines in Multi-Bus Power System Architectures," in *IEEE Transportation Electrification Conference & Expo (ITEC)*, Chicago, 2020.

[15] O. Tremblay, L. A. Dessaint and A. I. Dekkiche, "A generic battery model for the dynamic simulation of hybrid electric vehicles," in *IEEE Vehicle Power and Propulsion Conference*, Arlington, 2007.

[16] K. E. Yeager and J. R. Willis, "Modeling of emergency diesel generators in an 800 megawatt nuclear power plant," *IEEE Transactions on Energy Conversion,* vol. 8, no. 3, pp. 433-441, 1993.

[17] L. J. Rashkin, J. C. Neely, S. F. Glover, T. J. McCoy and S. D. Pekarek, "Dynamic considerations of power system coupling through dual-wound generators," in *2017 IEEE Electric Ship Technologies Symposium (ESTS)*, Arlington, 2017.

[18] M. A. Abkowitz, "Stability and Motion Control of Ocean Vehicles," The M.I.T. Press, Cambridge, 1969.

[19] D. W. Baker and C. L. Patterson, "Represenentation of Propeller Thrust and Torque Characteristics for Simulations: Appendix C: Data for 18 Propellers," Naval Ship Research and Development Center, West Bethesda, 1970.

[20] D. W. Baker and C. L. Patterson, "Representation of Propeller Thrust and Torque Characteristics for Simulations," Naval Ship Research and Development Center, West Bethesda, 1968.